Consistency Analysis for the Doubly Stochastic Dirichlet Process

Xing Sun, *Student Member, IEEE,* Nelson H.C. Yung, *Senior Member, IEEE,* Edmund Y. Lam, *Fellow, IEEE,* and Hayden K.-H. So, *Senior Member, IEEE*

arXiv:1605.07358v1 [cs.IT] 24 May 2016

Abstract

This technical report proves components consistency for the Doubly Stochastic Dirichlet Process [1] with exponential convergence of posterior probability. We also present the fundamental properties for DSDP as well as inference algorithms. Simulation toy experiment and real-world experiment results for single and multi cluster also support the consistency proof. This report is also a support document for the paper "Computationally Efficient Hyperspectral Data Learning Based on the Doubly Stochastic Dirichlet Process" [1].

Index Terms

Bayesian model, Consistency for number of components

I. The asymptotic mass function and exchangeable partitions

The probability of data partitions is important in mixture modeling [2]. Let $\mathcal{M}$ be the unordered partition of n observations, then the probability mass function [3] of $\mathcal{M}$ follows.

Lemma I.1. *Let D denote a DSDP-MM with a Marked SGP prior thinning function $q'(\boldsymbol{\theta}_k, n_k) = q(\boldsymbol{\theta}_k) \times Q(n_k)$. The probability mass function of the unordered data partition $\mathcal{M}$ follows*

$$P(\mathcal{M}) = \frac{(\alpha^*)^K \Gamma(\alpha^*)}{\Gamma(\alpha^* + n)} \cdot \prod_{k=1}^{K} \Big\{ \Gamma(n_k) \cdot Q(n_k) \Big\}, \tag{1}$$

X. Sun, E. Lam, and H. So are with the Department of Electrical and Electronic Engineering, The University of Hong Kong, Pokfulam, Hong Kong (email: hso@eee.hku.hk).

N. Yung is with Yung & Partners Limited, Hong Kong.

Manuscript received May, 2016

where n_k is the number of k^{th} data partition with the topic $\boldsymbol{\theta}_k$, and the number of land-cover classes is denoted as K.

Let $\mathcal{M}^r = (\mathcal{M}_1^r, \ldots, \mathcal{M}_{|\mathcal{M}|}^r)$ be the ordered derivation of random partition $\mathcal{M}$, and the order is uniformly sampled from all $|\mathcal{M}|!$ possible choices [4]. Let random vector $\mathcal{N} = (\mathcal{N}_1, \ldots, \mathcal{N}_{|\mathcal{M}|})$ be the size vector of $\mathcal{M}^r$ and $\boldsymbol{n} = (n_1, \ldots, n_K)$, then the ordered partition probability follows

$$\begin{aligned} P(\mathcal{N} = \boldsymbol{n}) &= \sum_{\mathcal{M}^r : \mathcal{N}(\mathcal{M}^r) = \boldsymbol{n}} \frac{P(\mathcal{M})}{|\mathcal{M}|!} \\ &= \frac{n!}{K!} \frac{B(n)^K}{\Gamma(a_0)^K} \frac{{b_0}^{K \cdot a_0} n^n}{(b_0 + n)^{K \cdot a_0 + n}} \frac{{\alpha^*}^K \Gamma(\alpha^*)}{\Gamma(\alpha^* + n)} \prod_{k=1}^{K} \frac{\Gamma(a_0 + n_k)}{n_k \cdot n_k!}. \end{aligned} \tag{2}$$

To obtain asymptotic partition probability, the asymptotic marked function is derived first.

Lemma I.2. *For any cluster amount $K \in \{1, 2, \ldots\}$ and any finite hyper-parameter $a_0 > 0$, if the mixture weight of the partition would always be nonzero $\frac{n_{\boldsymbol{\theta}}}{n} > 0$, as the data amount grows $n \to \infty$, the asymptotic marked function follows*

$$Q(n_{\boldsymbol{\theta}}) \sim \frac{(n_{\boldsymbol{\theta}} + 1)^{a_0 - 1}}{n^{a_0}}. \tag{3}$$

As $n \to \infty$, the ordered partition probability follows

$$P(\mathcal{N} = \boldsymbol{n}) \sim \frac{(\alpha^* b_0^{a_0})^K}{e \cdot n^{(\alpha^* + K \cdot a_0)} \cdot \Gamma(a_0)^K} \cdot \frac{n!}{K!} \cdot \prod_{k=1}^{K} n_k^{(a_0 - 2)}. \tag{4}$$

When the number of partitions $|\mathcal{M}|$ is given, the conditional partition size probability $P(\mathcal{N} = \boldsymbol{n} \mid |\mathcal{M}| = K)$ of DSDP Mixture P_{DS}, the Mixture of Finite Mixture (MFM) P_{FM} [4] and the DP Mixture P_{DP} follows

$$P_{DS} \propto \prod_{k=1}^{K} n_k^{(a_0 - 2)}, P_{FM} \propto \prod_{k=1}^{K} n_k^{(\gamma - 1)}, P_{DP} \propto \prod_{k=1}^{K} n_k^{-1}, \tag{5}$$

where γ is the hyper-parameter for MFM. When $a_0 = \gamma + 1$, the size probability P_{DS} of DSDP is the same as P_{FM} of the MFM. The size probability P_{DS} is equal to P_{DP} of the DP when $a_0 = 1$. Overall, Eq. 5 illustrates that all of these three models are shaped as a symmetric K-dimensional Dirichlet distribution, and the partition is exchangeable.

Discussions above assume that the weight of each partition is nonzero, as the correct mixture weights are nonzero. Here, a general situation in HSI identification is discussed, where some partition amounts (HSI data amounts of some land-cover classes) may be quite small.

Lemma I.3. *For any partition amount $n_{\boldsymbol{\theta}} \geq 1$, any cluster amount $K \in \{1, 2, \ldots\}$and any finite hyper-parameter $a_0 > 0$, as $n \to \infty$, asymptotic marked function follows*

$$Q(n_{\boldsymbol{\theta}}) \sim \frac{\Gamma(a_0 + n_{\boldsymbol{\theta}})}{\Gamma(a_0)\Gamma(n_{\boldsymbol{\theta}})} \cdot \frac{{n_{\boldsymbol{\theta}}}^{-1}}{(n + b_0)^{a_0}}. \tag{6}$$

This lemma is more general for any partition amount $n_{\boldsymbol{\theta}}$.

Theorem I.4. *For any sampled partition size $n_k \in \mathbb{Z}^+, k = 1, \ldots, K$, when number of clusters is given with $|\mathcal{M}| = K$, the conditional partition size probability of DSDP-MM follows*

$$P\Big(\mathcal{N} = \boldsymbol{n} \big| |\mathcal{M}| = K\Big) \propto \prod_{k=1}^{K} n_k^{-1} \frac{\Gamma(a_0 + n_k)}{\Gamma(a_0)\Gamma(n_k)}. \tag{7}$$

II. Consistency theorem proof

First, the following proof is based on the background knowledge of the conjugate prior in [5]. Suppose that the observation $\boldsymbol{X}$ is sampled from an exponential family distribution $p_{\boldsymbol{\theta}}(\boldsymbol{x}_j)$, then $T_1(\boldsymbol{x}_j)$, $h_0(\boldsymbol{\theta})$ and $A_1(\boldsymbol{\theta})$ are the sufficient statistic, the underlying measure and the log normalization, respectively. The natural parameter $\eta_0 = \langle \eta_1, \eta_2 \rangle$ is the hyper-parameter of the base distribution $H_0(\boldsymbol{\theta}|\eta_0)$.

Second, to derive probabilities $\boldsymbol{p}$ and $\boldsymbol{q}$, a marginal probability of DSDP-MM follows

$$m_q(\vec{\boldsymbol{x}}_{\mathrm{A}_i}) = \int_{\Theta} H_0(\boldsymbol{\theta}) \sigma\left(Y(\boldsymbol{\theta})\right) \prod_{j \in \mathrm{A}_i} p(\boldsymbol{x}_j|\boldsymbol{\theta}) \mathrm{d}\boldsymbol{\theta} = \prod_{j \in \mathrm{A}_i} p_0(\boldsymbol{x}_j) \cdot \int_{\Theta} e^{\eta_{\mathrm{A}_i} f_{\mathrm{A}_i}(\boldsymbol{\theta})} \sigma\left(Y(\boldsymbol{\theta})\right) \mathrm{d}\boldsymbol{\theta}, \tag{8}$$

where $\eta_{\mathrm{A}_i} = (\eta_2 + |\mathrm{A}_i|)$ is the natural parameter for the data partition A_i. The function follows $f_{\mathrm{A}_i}(\boldsymbol{\theta}) = \boldsymbol{\mu}_{\mathrm{A}_i}^T \boldsymbol{\theta} - A_1(\boldsymbol{\theta}) + \eta_{\mathrm{A}_i}^{-1} \log(h_0(\boldsymbol{\theta}))$, where $\boldsymbol{\mu}_{\mathrm{A}_i} = \eta_{\mathrm{A}_i}^{-1}(\sum_{j \in \mathrm{A}_i} T_1(\boldsymbol{x}_j) + \eta_1)$.

Subsequently, observations in the newly separated cluster have the same original topic, as the Split-Merge MCMC is applied. The extra partition is the subset of a original data partition $\mathrm{A}_{K+1} \subset \mathrm{B}_i, i \leq K$. The data partition probability in Theorems V.1 and V.2 in [1] is derived as

$$\begin{aligned} P\left(T_n = K, \boldsymbol{x}_{1:n}\right) =& \sum_{\mathrm{B} \in \mathrm{A}_K(n)} p(\mathrm{B}) \prod_{i=1}^{K} m_q(\vec{\boldsymbol{x}}_{\mathrm{B}_i}) \\ =& \frac{c_\Gamma c_Q N_{\{\mathrm{B} \to \mathrm{A}\}}}{|\mathcal{R}_{\mathrm{A}}(\mathcal{M}, \mathcal{C}_\varphi)|} \times \sum_{\mathrm{A} \in \mathrm{A}_{K+1}(n)} c_\varphi(\mathrm{A}) p(\mathrm{A}) \prod_{i=1}^{K+1} m_q(\vec{\boldsymbol{x}}_{\mathrm{A}_i}) \\ =& C_\Phi \cdot p\left(T_n = K + 1, \boldsymbol{x}_{1:n}\right), \end{aligned} \tag{9}$$

where $c_\Gamma c_Q$ are mass and marked function ratios defined in Eq. 10 in the Section III. The $\mathcal{R}_{\mathrm{A}}(\mathcal{M}, \mathcal{C}_\varphi)$ is the set of all possible new partitions A_{K+1} such that its parent partition A_l satisfies $m_q(\vec{\boldsymbol{x}}_{\mathrm{A}_l}) = c_\varphi m_q(\vec{\boldsymbol{x}}_{\mathrm{A}_{K+1}}) m_q(\vec{\boldsymbol{x}}_{\mathrm{A}_l \setminus \mathrm{A}_{K+1}})$ for all $\mathrm{A} \in \mathrm{A}_{K+1}(n)$, which subjects to $c_\varphi(\mathrm{A}) \in \mathcal{C}_\varphi$.

Lastly, based on partition probability, four cases are provided to prove Theorems V.1 and V.2 in [1].

1) First, if the sampled data partition amount K is correct in the previous iteration $(t-1)$, then it is impossible that any original data partition B_l would split into two partitions A_l, A_{K+1} at current iteration (t) when $p(T_n^{(t-1)} = K) \geq cn^{s_0} p(T_n^{(t)} = K+1)$. This equation is satisfied with the conclusion $P_n(C_\Phi \geq cn^{s_0}) = 1$, which is shown in III-B1.
2) The second case shows the situation that the partition amount $K+1$ has been correctly sampled in the previous iteration $(t-1)$. Then it is impossible that two partitions A_l, A_{K+1} would merge when $p(T_n^{(t)} = K) \leq cn^{-v_0} p(T_n^{(t-1)} = K+1)$. See the conclusion $P_n(C_\Phi \leq cn^{-v_0}) = 1$ in III-C2 for details.
3) Third, if the sampled partition amount $K+1$ in the previous iteration $(t-1)$ is larger than actual amount K, there exists a nonzero possibility that two partitions A_l, A_{K+1} would merge at this iteration (t) when $p(T_n^{(t)} = K) \geq c \cdot p(T_n^{(t-1)} = K+1)$. The conclusion $P_n(C_\Phi \geq c) = 1$ in III-B2 explains details.
4) Lastly, if the situation that the sampled partition amount K in the previous iteration $(t-1)$ is smaller than the actual amount $K+1$, there exists the possibility that a partition B_l would split into two partitions A_l, A_{K+1} at this iteration (t) when $p(T_n^{(t-1)} = K) \leq c \cdot p(T_n^{(t)} = K+1)$. It is satisfied with the conclusion $P_n(C_\Phi \leq c) = 1$ in III-C1.

III. Posterior Probability Ratios and Conditions

In Eq. 9, coefficient C_Φ contains five major elements.

The first two elements are the mass coefficient c_Γ, and the marked coefficient c_Q, which are derived with the Eq. 6,

$$c_\Gamma c_Q = \frac{|\vec{\boldsymbol{x}}_{\mathrm{A}_l}|^{\frac{3}{2}} |\vec{\boldsymbol{x}}_{\mathrm{A}_{K+1}}|^{\frac{3}{2}}}{|\vec{\boldsymbol{x}}_{\mathrm{B}_l}|^{\frac{3}{2}} (n+b_0)^{-a_0}} \frac{\Gamma(a_0)\Gamma(a_0 + |\vec{\boldsymbol{x}}_{\mathrm{B}_l}|)}{\Gamma(a_0 + |\vec{\boldsymbol{x}}_{\mathrm{A}_l}|)\Gamma(a_0 + |\vec{\boldsymbol{x}}_{\mathrm{A}_{K+1}}|)}. \tag{10}$$

The third factor $N_{\{\mathrm{B}\to\mathrm{A}\}}$ is the number of possible partitions $\mathrm{B} \in \mathrm{A}_K(n)$ that splitting into $\mathrm{A} \in \mathrm{A}_{K+1}(n)$. In the Algorithm 2, A_{K+1} is the subset of one original partition, where at most K possibilities. Therefore, $N_{\{\mathrm{B}\to\mathrm{A}\}} \in \{0, 1, \ldots, K\}$.

The fourth element is the marginal probability ratio c_φ, for any partition $\mathrm{A} \in \mathrm{A}_{K+1}(n)$, the ratio follows

$$c_\varphi(\mathrm{A}) = \frac{m_q(\vec{\boldsymbol{x}}_{\mathrm{A}_l}) m_q(\vec{\boldsymbol{x}}_{\mathrm{A}_{K+1}})}{m_q(\vec{\boldsymbol{x}}_{\mathrm{B}_l})} \tag{11a}$$

$$= c_Y \frac{\int_\Theta e^{\eta_{\mathrm{A}_l} f_{\mathrm{A}_1}(\boldsymbol{\theta})} \mathrm{d}\boldsymbol{\theta} \cdot \int_\Theta e^{\eta_{\mathrm{A}_{K+1}} f_{\mathrm{A}_{\mathrm{K+1}}}(\boldsymbol{\theta})} \mathrm{d}\boldsymbol{\theta}}{\int_\Theta e^{\eta_{\mathrm{B}_l} f_{\mathrm{B}_\mathrm{l}}(\boldsymbol{\theta})} \mathrm{d}\boldsymbol{\theta}} \tag{11b}$$

$$= c_Y c_L \omega_r \prod_{i=l,K+1} e^{-\eta_{\mathrm{A}_i} || f_{\mathrm{A}_\mathrm{i}}(\boldsymbol{\theta}^*_{\mathrm{A}_\mathrm{i}}) - f_{\mathrm{A}_\mathrm{i}}(\boldsymbol{\theta}^*_{\mathrm{B}_\mathrm{l}}) ||}, \tag{11c}$$

where $\omega_r = \frac{\sqrt{\eta_{\mathrm{B}_l}}}{\sqrt{\eta_{\mathrm{A}_l} \eta_{\mathrm{A}_{K+1}}}}$, and c_Y, c_L are finite constants. Eq. 11 (b) is the ratio for normalized constant. Coefficient $c_Y > 0$ is finite when SGP function $\sigma\left(Y(\boldsymbol{\theta})\right)$ is removed, which is shown in Section IV. In Eq. 11 (c), Laplace's method [6] has been applied to approximate the normalization constant. The function $f(\boldsymbol{\theta})$ is the posterior probability of the parameter $\boldsymbol{\theta}$, and the extreme value location $\boldsymbol{\theta}^*$ is the topic of any data set $\boldsymbol{x}_s$. For the Laplace's method, the function $f(\boldsymbol{\theta})$ is second-order differentiable and its second order derivative at $\boldsymbol{\theta}^*$ follows $f''(\boldsymbol{\theta}^*) < 0$, due to that $f''(\boldsymbol{\theta}^*) = -\mathrm{var}(\boldsymbol{x}_s)$ [7].

The last factor is the possible partition amount $|\mathcal{R}_\mathrm{A}(\mathcal{M}, \mathcal{C}_\varphi)|$, which is discussed in Section III-B and Section III-C.

A. The finite mixture weight condition

Condition III.1. If there exists a finite DP Mixture weight prior $\pi_0(\boldsymbol{\theta}) < \infty, \forall \boldsymbol{\theta} \in \Theta$, the topic parameter or data partition amount is finite. As the whole data amount grows, for any sample data partition $\boldsymbol{X}_\mathrm{B}$, its amount $|\mathrm{B}|$ follows that

$$\lim_{n \to \infty} P(\frac{|\mathrm{B}|}{n} > 0) = 1. \tag{12}$$

B. Data partitions with the same topic parameter

Based on the Slutsky's theorem [8], if observations are sampled from distributions with the same topic $\boldsymbol{\theta}_0$, as the data amount $|\mathrm{A}| \to \infty$, inferred topic parameters $\boldsymbol{\theta}^*_\mathrm{A}$ of any sampled data partition A will approach the real topic $\boldsymbol{\theta}_0$, i.e.

$$\boldsymbol{\theta}^*_\mathrm{A} = A_1'^{-1} \left(\frac{1}{|\mathrm{A}|} \sum_{i \in \mathrm{A}} T_1(\boldsymbol{X}_i) \right) \xrightarrow{P} \boldsymbol{\theta}_0, \tag{13}$$

where $A_1^{'-1}$ is the inverse function of the derivative of the log normalization. See [7] for detailed asymptotic properties. Hence, for any two data partitions A and B, whose data are sampled from the same topic $\boldsymbol{\theta}_0$ with Condition III.1. The function f_{A} in Eq. 11 can be derived under this setting. As data amount grows, there exists a constant $c > 0$, which subjects to

$$\begin{aligned} P\big\{||\boldsymbol{\theta}^*_{\mathrm{A}} - \boldsymbol{\theta}^*_{\mathrm{B}}|| < \frac{c}{\min\{|\mathrm{A}|, |\mathrm{B}|\}}\big\} = 1, \\ P\big\{||f_{\mathrm{A}}(\boldsymbol{\theta}^*_{\mathrm{A}}) - f_{\mathrm{A}}(\boldsymbol{\theta}^*_{\mathrm{B}})|| < \frac{c}{|\mathrm{B}|}\big\} = 1, \end{aligned} \tag{14}$$

where $\boldsymbol{\theta}^*_{\mathrm{A}}, \boldsymbol{\theta}^*_{\mathrm{B}}$ are inferred topics for data partition A and B.

Let $w_{\mathrm{A}} = a_0 + |\vec{\boldsymbol{x}}_{\mathrm{A}}| - 1$ for any data partition A. If data partitions are sampled from the same topic, two situations are discussed with the amount of data partition $w_{\mathrm{A}_{K+1}}$ is finite: finite split with a correctly inferred SGP prior, and finite merge with a incorrectly inferred SGP prior. The possible partition number follows $|\mathcal{R}_{\mathrm{A}}(\mathcal{M}, \mathcal{C}_\varphi)| \leq (w_{\mathrm{A}_{K+1}})! = c_g$, and it is finite at these situations when $w_{\mathrm{A}_{K+1}}$ is finite. Hence, the coefficients C_Φ can be derived, with

$$\lim_{n\to\infty} C_\Phi = C_1 \cdot \bar{c}_\varphi n^{(w_{\mathrm{A}_{K+1}}+1)}, \tag{15}$$

where $C_1 = \frac{|\vec{\boldsymbol{x}}_{\mathrm{A}_{K+1}}|^{\frac{3}{2}}\Gamma(a_0)}{c_g\Gamma(w_{\mathrm{A}_{K+1}}+1)} > 0$ is finite. The mean ratio $\bar{c}_\varphi$ is the weighting average for all data partitions $\mathrm{A} \in \mathrm{A}_{K+1}(n)$ in Eq. 9. This derivation is based on substituting Eq. 10 and the Gamma function ratio $\lim_{n\to\infty} \frac{\Gamma(a_0+|\vec{\boldsymbol{x}}_{\mathrm{B}_l}|)}{\Gamma(a_0+|\vec{\boldsymbol{x}}_{\mathrm{A}_l}|)} = cn^{|\mathrm{A}_{K+1}|}$ into Eq. 9, in which $c > 0$ is a finite constant.

Substituting Eq. 14 into Eq. 11, then for any partition $\mathrm{A} \in \mathrm{A_{K+1}(n)}$, the ratio $c_\varphi(\mathrm{A})$ can be derived from Eq. 15, where

$$\begin{aligned} &\lim_{n\to\infty} P_n(C_\Phi \geq cn^{s_0}) \\ &\quad = \lim_{n\to\infty} P_n\left(c_\varphi(\mathrm{A}) > c \cdot \frac{n^{(s_0 - w_{\mathrm{A}_{K+1}})}}{|\mathrm{B}|}\right) = 1. \end{aligned} \tag{16}$$

The value of the variable s_0 determines which situation Eq. 16 is suitable.

1) Finite Split: $s_0 = w_{\mathrm{A}_{K+1}} > 0$. Partition B_l is impossible to split into two partitions A_l, A_{K+1} at this iteration (t), when sampling in the previous iteration is correct.

2) Finite Merge: $s_0 = 0$. The probability that merges two sampled partitions A_l and A_{K+1} in the previous iteration step to compose a correct new partition B_l is larger than zero.

Discussion for infinite split with the correct SGP prior and infinite merge with the incorrect SGP prior are quite similar.

C. Data partitions with different topic parameters

For any two data partitions A, B, whose observations are sampled from two different topics $\boldsymbol{\theta}_{a0}, \boldsymbol{\theta}_{b0}$ with $||\boldsymbol{\theta}_{a0} - \boldsymbol{\theta}_{b0}|| > 0$. As the data amounts of these two partitions grow, there exists a finite constant $c > 0$, which subjects to

$$\begin{aligned} P\Big(||\boldsymbol{\theta}^*_{\mathrm{A}} - \boldsymbol{\theta}^*_{\mathrm{B}}|| > c\Big) = 1 \\ P\Big(||f_{\mathrm{A}}(\boldsymbol{\theta}^*_{\mathrm{A}}) - f_{\mathrm{A}}(\boldsymbol{\theta}^*_{\mathrm{B}})|| > c\Big) = 1, \end{aligned} \tag{17}$$

where $\boldsymbol{\theta}^*_{\mathrm{A}}, \boldsymbol{\theta}^*_{\mathrm{B}}$ are estimated topics (maximum posterior parameters) for data partitions A and B, respectively.

In this situation, we discuss partitions, which have finite and nonzero mixture weight. The amount ratios follow that $\lim\limits_{n\to\infty} \frac{w_{\mathrm{A}_{K+1}}}{w_{\mathrm{B}_l}} = c_1 > 0$, $1 - c_1 = \lim\limits_{n\to\infty} \frac{w_{\mathrm{A}_l}}{w_{\mathrm{B}_l}} > 0$. The possible partition number follows $|\mathcal{R}_{\mathrm{B}}(\mathcal{M}, \mathcal{C}_\varphi)| > 1$ at these situations. The coefficients C_Φ can be derived with the asymptotic expression, $\Gamma(w_{\mathrm{B}_l} + 1) \sim \sqrt{2\pi w_{\mathrm{B}_l}}\big(\frac{w_{\mathrm{B}_l}}{e}\big)^{w_{\mathrm{B}_l}}$.

$$\begin{aligned} \lim_{n\to\infty} C_\Phi &= \frac{C_1 \cdot \bar{c}_\varphi |\vec{\boldsymbol{x}}_{\mathrm{B}_l}|^{(a_0+\frac{3}{2})} \sqrt{2\pi w_{\mathrm{B}_l}} \big(\frac{w_{\mathrm{B}_l}}{e}\big)^{w_{\mathrm{B}_l}}}{2\pi \sqrt{w_{\mathrm{A}_l} w_{\mathrm{A}_{K+1}}} \big(\frac{w_{\mathrm{A}_l}}{e}\big)^{w_{\mathrm{A}_l}} \big(\frac{w_{\mathrm{A}_{K+1}}}{e}\big)^{w_{\mathrm{A}_{K+1}}}} \\ &= C_2 \cdot \bar{c}_\varphi |\vec{\boldsymbol{x}}_{\mathrm{B}_l}|^{(a_0+1)} \cdot {c_u}^{w_{\mathrm{B}_l}}, \end{aligned} \tag{18}$$

where $C_1 = \Gamma(a_0)(c_1 - c_1^2)^{1.5} \frac{(n+b_0)^{a_0}}{w_{\mathrm{B}_l}^{a_0}}$ is finite with Condition III.1, and $C_2 = \frac{e}{\sqrt{2\pi(c_1 - c_1^2)}} C_1$. The mean ratio $\bar{c}_\varphi$ is the weighting average for all data partitions $\mathrm{B} \in \mathrm{B}_K(n)$ in Eq. 9. This derivation is based on substituting Eq. 10 and the Gamma function ratio: $\{(c_1)^{-c_1}(1-c_1)^{-1+c_1}\}^{w_{\mathrm{B}_l}}$ into Eq. 9. Since $c_1 \in (0, 1)$, the constant $c_u \in (1, 2)$. Substitute Eq. 17 into Eq. 11, then for any partition $\mathrm{B} \in \mathrm{B_K(n)}$, the ratio $c_\varphi(\mathrm{B})$ can be further derived from Eq. 18, where

$$\begin{aligned} &\lim_{n\to\infty} P_n(C_\Phi \leq c n^{-v_0}) \\ &\quad = \lim_{n\to\infty} P_n(c_\varphi(\mathrm{B}) < 2^{-\mathrm{w_{B_l}}} |\tilde{\boldsymbol{x}}_{\mathrm{B_l}}|^{-(\mathrm{v_0}+\mathrm{a_0}+1)}) = 1. \end{aligned} \tag{19}$$

Two situations of the variable v_0 in Eq. 19 require further comments.

1) Infinite Split: $v_0 = 0$. The probability that split an incorrect partition B_l into two partitions A_l and A_{K+1} is larger than zero.

2) Infinite Merge: $v_0 > 0$. The probability that merge two correctly sampled partitions A_l and A_{K+1} in the previous iteration step to compose a new partition B_l is zero.

Discussions for finite merge with the correct SGP prior and finite split with the incorrect SGP prior are not provided, as these two situations do not exist based on Condition III.1.

IV. Gaussian Process Intensity

To maximize the likelihood in Eq. 9 in [1], the likelihood $\ln p(\boldsymbol{Y}, |\vec{\boldsymbol{\theta}}, M, K)$ can be set to zero. Then we can obtain $\boldsymbol{Y}_{K+M} = \boldsymbol{\Sigma}_{(K+M)\times(K+M)}[\sigma(-Y_1)\ldots-\sigma(Y_{K+M})]^T$. Here we introduce two variables used for sampling the SGP Cox Process [9]. The variable a_{ins} indicates the probability to add a new latent variable with the corresponding GP function Y_{new} and the variable a_{del} is the probability to delete an existing latent variable with Y_{old}. Increase and delete ratios will be balanced at $a_{ins} = a_{del}$ when the convergence is achieved. When we safely set the proposal probability $b(\cdot,\cdot) = 0.5$, the Condition III.1is satisfied for dataset $\boldsymbol{x}_{1:n}$, and the upper bound parameter α^* is finite, we can conclude amounts of the topic parameters and latent variables follow

$$\lim_{n\to\infty} \sup_{c\in(0,1)} P\left((K+M) < c\alpha^*\right) = 1. \tag{20}$$

For any latent topic parameter $\boldsymbol{\theta}_k \in \boldsymbol{\theta}_{1:K}$, the corresponding GP function Y_k can be derived as

$$Y_k = \sum_{i=1}^{K} \frac{e^{(-Y_i)} k\left(\boldsymbol{\theta}_k, \boldsymbol{\theta}_i\right)}{1+e^{(-Y_i)}} - \sum_{i=K+1}^{K+M} \frac{k\left(\boldsymbol{\theta}_k, \boldsymbol{\theta}_i\right)}{1+e^{(-Y_i)}}. \tag{21}$$

The GP function Y_m of latent variable is similar. If K and M are finite, sampled GP functions follow $|Y_i| < \infty$, $i \in \{1,\ldots,K+M\}$. Therefore, the SGP function $\sigma(Y_i)$ follows

$$\lim_{n\to\infty} P\left(\sigma(Y_i) \in (0,1)\right) = 1. \tag{22}$$

Hence, for any data partition A_i, there always exists a finite constant $c > 0$, which subject to

$$\frac{\int_\Theta e^{\eta_{\mathrm{A}_i} f_{\mathrm{A}_\mathrm{i}}(\boldsymbol{\theta})} \mathrm{d}\boldsymbol{\theta}}{\int_\Theta e^{\eta_{\mathrm{A}_i} f_{\mathrm{A}_\mathrm{i}}(\boldsymbol{\theta})} \sigma\left(Y(\boldsymbol{\theta})\right) \mathrm{d}\boldsymbol{\theta}} = c. \tag{23}$$

V. Algorithms

Here, we present two algorithms: Assignment Sampling for each HSI pixel $\boldsymbol{x}_i$ for DSDP-MM and Split-Merge MCMC Algorithm for DSDP-MM, which are shown in Algorithm 1 and Algorithm 2, respectively.

VI. Experiment

A. Single Cluster Simulation

The density sampling inference of DPMM may achieve consistent when the data amount grows, but the inconsistency problem still exists for the number of clusters. Moreover, this

Algorithm 1 Assignment Sampling for each HSI pixel $\boldsymbol{x}_i$ for DSDP-MM with the Marked SGP prior

Input: Likelihood $\ell(\boldsymbol{x}_i|\boldsymbol{\theta}_{k,i})$, data amount $n_{-i,k}$ and GP functions $Y_{1:K+M}^{(t)}$

Output: Assignment sample $\vec{z}_i^{(t+1)}$

for $k = 1 : K$ **do**

    Calculate the thinning function: $q(\boldsymbol{\theta}_k, n_{\boldsymbol{\theta}_k}) \propto n_{-i,k} \cdot \sigma(Y_k) \cdot \dfrac{Q(n_{-i,k}+1)}{Q(n_{-i,k})}$

end for

for $k = K+1 : K+M$ **do**

    Calculate the thinning function: $q(\boldsymbol{\theta}_k, n_{\boldsymbol{\theta}_k}) \propto \dfrac{\alpha^*}{M} \cdot \sigma(Y_k) \cdot Q(1)$

end for

Sample assignment $\vec{z}_i^{(t+1)}$ via Eq. 11 in [1]

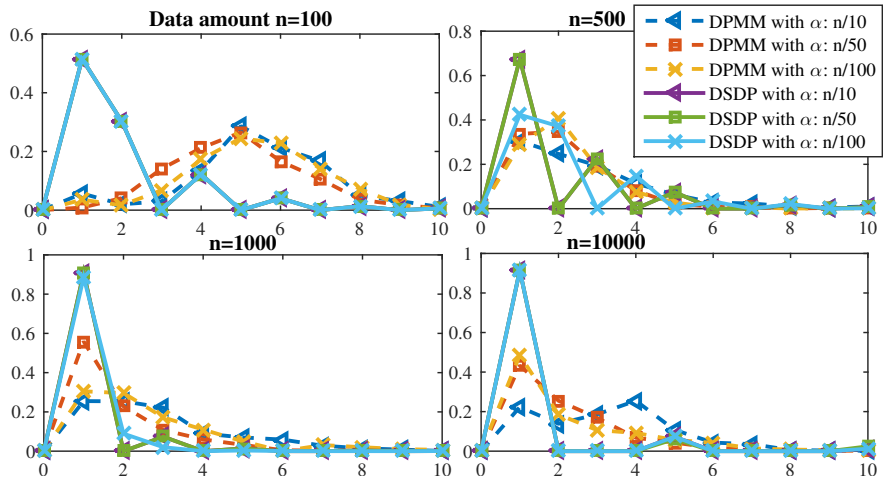

Fig. 1: Posterior probabilities of the cluster number with various initial concentration parameters α^*. Clustering is applied on a single simulation dataset by DPMM and DSDP-MM.

inconsistency problem could be severe for the single cluster dataset. For a robust nonparametric Bayesian mixture model, it is important that the cluster number could be consistent with different values of the initial concentration parameter and the data amount. Therefore, this simulation experiment is built based on the following points:

1) For the number of clusters, we applied the single cluster simulation data, which is the most severe inconsistency problem in [10].

Algorithm 2 Split-Merge MCMC Algorithm for DSDP-MM with the Marked SGP prior (Split case)

Random sample two data x_i and x_j ▷ Stage 1

Let sampled distinct observation x_i and x_j crate two new cluster $\mathcal{S}_1^{(0)}, \mathcal{S}_2^{(0)}$ respectively

Let $\mathcal{S}_{\boldsymbol{c}}$ be the set of data which are belonged to z_i or z_j excluding x_i and x_j in state $\boldsymbol{c}$

let $t \leftarrow 0$ ▷ Stage 2

Randomly permute $\mathcal{S}_{\boldsymbol{c}}$ with the random order function $\tau(\cdot)$

if $z_i = z_j = k$ **then** ▷ Split case

  $T(\boldsymbol{c} \to \boldsymbol{c}_{split}) \leftarrow 1, \qquad T(\boldsymbol{c}_{split} \to \boldsymbol{c}) \leftarrow 1$

  for random order $m \in \tau(1), ..., \tau(|\mathcal{S}_{\boldsymbol{c}}|)$ **do**

    Assignment sampling $z_m^r \sim p(z_m | \mathcal{S}_1^{(t)}, \mathcal{S}_2^{(t)})$

    $T(\boldsymbol{c} \to \boldsymbol{c}_{split}) \leftarrow T(\boldsymbol{c} \to \boldsymbol{c}_{split}) p(z_m = z_m^r | \mathcal{S}_1^{(t)}, \mathcal{S}_2^{(t)}) \prod_{l=1,2} \frac{T\left(\boldsymbol{\theta}_{\mathcal{S}_l^{(t)}} \to \boldsymbol{\theta}_{\mathcal{S}_l^{(t-1)}}\right)}{T\left(\boldsymbol{\theta}_{\mathcal{S}_l^{(t-1)}} \to \boldsymbol{\theta}_{\mathcal{S}_l^{(t)}}\right)}$

  end for

  Calculate the acceptance ratio $\mathcal{A} \leftarrow \frac{PG\ell(\boldsymbol{c}_{split}) Q(|\boldsymbol{c}_{split}|) T(\boldsymbol{c}_{split} \to \boldsymbol{c})}{PG\ell(\boldsymbol{c}) Q(|\boldsymbol{c}|) T(\boldsymbol{c} \to \boldsymbol{c}_{split})}$

  $t \leftarrow t + 1$

else

..... ▷ Merge case

end if

Sample $u \sim \text{Unif}(0, 1)$, if $u < \mathcal{A}$, accept the move; otherwise, reject it.

2) For the initial hyper-parameter, three typical values have been used: $n/10, n/50$ and $n/100$.

3) For the data amount, we analyze the range from 10^2 to 10^4, which is commonly used.

From Fig. 1, we can see that DPMM has severe inconsistency problem for the single cluster data [10], but the proposed DSDP-MM can obtain a consistent result even for this situation. In this simulation, different initial concentration parameters α have been used. The x-axis in Fig. 1 shows the number of clusters. The y-axis represents the frequency of the number of clusters occurring in the last 1000 iterations after convergence.

First, we discuss experimental results with various data amounts, four panels represent four different values of the data amount from 100 to 10000. When the data amount is small, such as $n = 100$ and $n = 500$, the inconsistency becomes serious, especially for DPMM. DPMM

would wrongly infer the data partition and the posterior probability of the cluster number with any initial concentration parameter when the data amount follows $n = 100$. Subsequently, we employ different initial concentration parameters on all simulation data. When the data amount grows, such as $n = 1000$ and $n = 10000$ in bottom panels, posterior probabilities (dotted line) of DPMM become quite inconsistent for different α^*. In bottom panels, posterior probabilities (solid line) of DSDP-MM are consistent and closer to the ground truth. In conclusion, DSDP-MM obtains a more consistent data partition result compared to DPMM.

B. Galaxy Experiment

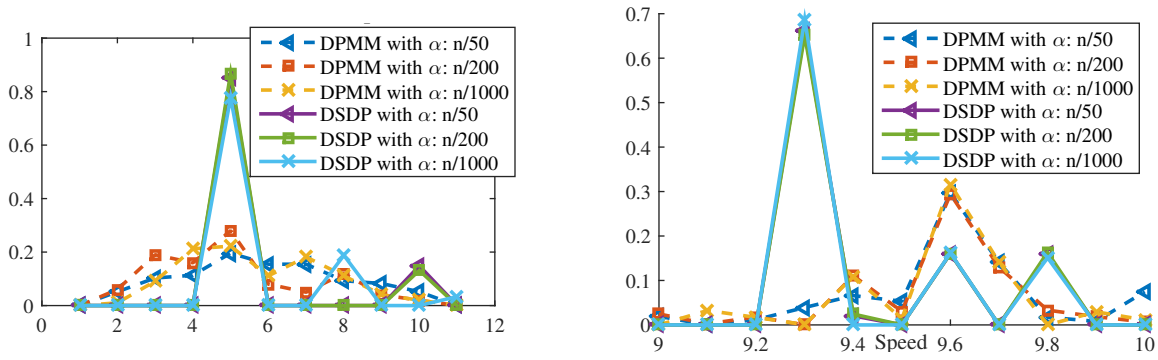

(a) Posterior probabilities of the cluster number

(b) The density of the Galaxy data

Fig. 2: Galaxy dataset clustering result for number of cluster and clusters density estimation

Here, we further experiment on the real-world galaxy data [1], which shows that DSDP-MM is adept in spatial clustering and estimating the density of the large-scale dataset. Shapley galaxy dataset with 4215 galaxies in the Shapley Concentration regions [11], which is used to illustrate the extensibility of DSDP-MM to other related spatial data without rich feature. Right ascension (Coordinate in the sky similar to longitude on Earth), Declination (Coordinate in the sky similar to latitude on Earth) and speed comprise the three-dimension feature space. This galaxy dataset is used to illustrate that DSDP-MM can achieve a consistent and robust result for large-scale dataset.

Fig. 2a also presents the posterior probabilities of the cluster number for DPMM and DSDP-MM, as the data amount n of this galaxy dataset is larger, we set the initial concentration

[1]This dataset can be downloaded at http://astrostatistics.psu.edu/datasets/Shapley_galaxy.html

parameter α^* with $n/10$, $n/200$ and $n/1000$. The posterior probabilities of DSDP-MM at the reasonable data partition $K = 5$ are all over 80% for various α^*, which are solid lines. Dotted lines show that posterior probabilities of DPMM are closer to the uniformly distribution and the sampling would be inconsistent. Therefore, this figure demonstrates that results of DSDP-MM are much more consistent than DPMM for the number of clusters.

Fig. 2b analyzes the density of the topic parameters in speed feature dimension. Since some topic parameters of the speed are closer, we plot the density with discretized interval 0.1. DSDP-MM also has a more robust density as the initial concentration parameters α^* decrease from $\alpha = n/50$ to $\alpha = n/1000$. Densities of DPMM (dotted lines) differ greatly with different α^*, especially for the speed from 9 to 9.4.

Fig. 3 presents the spatial clustering result of DPMM and DSDP with various α^*. Spatial clusters of DPMM are varying with different α^*, such as green, yellow and cyan clusters. Conversely, typical clusters of DSDP-MM in black, yellow and cyan, which are much robuster.

VII. Conclusion

Contributions can be regarded in two parts for this technical report: 1) we proved the consistency for the number of components in Doubly Stochastic Dirichlet process with exponential convergence of posterior probability. We have proved this model using single and multiple clusters experiments to support the consistency proof. 2) We have introduced theoretical properties of the Doubly Stochastic Dirichlet process with the Marked SGP prior.

References

[1] X. Sun, N. H. C. Yung, and E. Y. Lam, "Computationally efficient hyperspectral data learning based on the doubly stochastic dirichlet process," *IEEE TRANSACTIONS ON Geoscience and Remote Sensing*, p. Submitted, 2016.

[2] T. S. Ferguson, "A bayesian analysis of some nonparametric problems," *The Annals of Statistics*, pp. 209–230, 1973.

[3] C. E. Antoniak, "Mixtures of Dirichlet processes with applications to Bayesian nonparametric problems," *The Annals of Statistics*, pp. 1152–1174, 1974.

[4] J. W. Miller and M. T. Harrison, "Mixture models with a prior on the number of components," *arXiv preprint arXiv:1502.06241*, 2015.

[5] P. Diaconis, D. Ylvisaker *et al.*, "Conjugate priors for exponential families," *The Annals of Statistics*, vol. 7, no. 2, pp. 269–281, 1979.

[6] A. Azevedo-Filho and R. D. Shachter, "Laplace's method approximations for probabilistic inference in belief networks with continuous variables," in *UAI*, 1994, pp. 28–36.

[7] A. C. Davison, *Statistical Models*. Cambridge University Press, 2003.

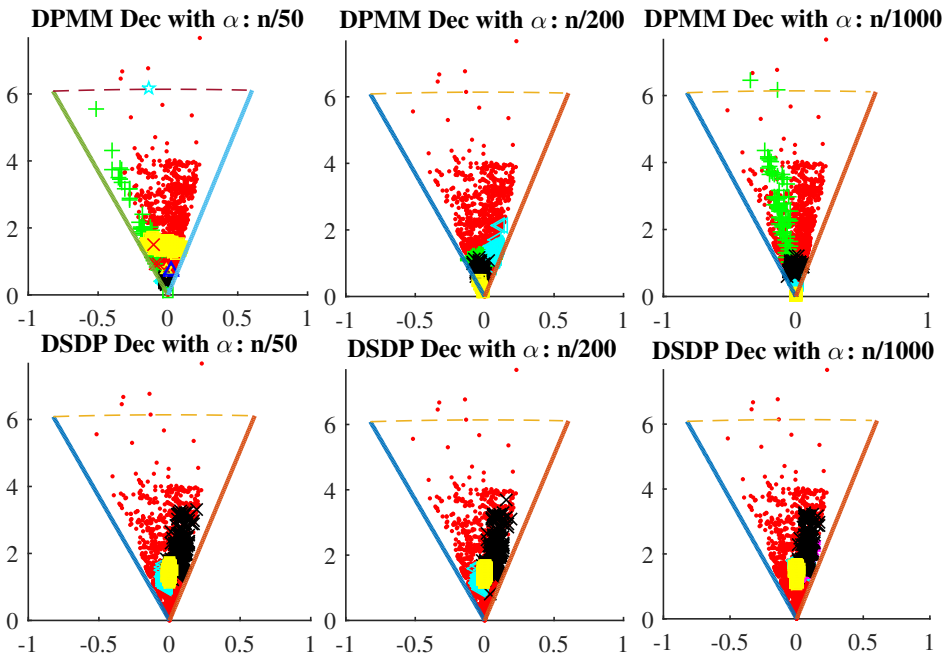
DPMM Dec with α: n/50
DPMM Dec with α: n/200
DPMM Dec with α: n/1000
DSDP Dec with α: n/50
DSDP Dec with α: n/200
DSDP Dec with α: n/1000

Fig. 3: Clustering result for Galaxy dataset with different concentration parameters. The angle θ indicates "Declination", which is the coordinate in the sky similar to latitude on Earth. The x-axis and y-axis show the Cartesian coordinates of the speed (diameter) and the declination (angle) with the scale $10^{-4} \cdot v \cos(\theta)$ and $10^{-4} \cdot v \sin(\theta)$ respectively.

[8] R. A. Bradley and J. J. Gart, "The asymptotic properties of ml estimators when sampling from associated populations," *Biometrika*, pp. 205–214, 1962.

[9] R. P. Adams, I. Murray, and D. J. MacKay, "Tractable nonparametric Bayesian inference in Poisson processes with Gaussian process intensities," in *International Conference on Machine Learning*, 2009, pp. 9–16.

[10] J. W. Miller and M. T. Harrison, "Inconsistency of Pitman-Yor process mixtures for the number of components," *The Journal of Machine Learning Research*, vol. 15, pp. 3333–3370, 2014.

[11] M. J. Drinkwater, Q. A. Parker, D. Proust, E. Slezak, and H. Quintana, "The large scale distribution of galaxies in the shapley supercluster," *Publications of the Astronomical Society of Australia*, pp. 89–96, 2004.